Purinergic Signalling (2010) 6:429–445
DOI 10.1007/s11302-010-9207-6

ORIGINAL ARTICLE

Purinergic receptor-mediated Ca^{2+} signaling in the olfactory bulb and the neurogenic area of the lateral ventricles

Thomas Hassenklöver · Philipp Schulz · Anna Peters · Peter Schwartz · Detlev Schild · Ivan Manzini

Received: 26 August 2010 / Accepted: 18 November 2010 / Published online: 1 December 2010

Abstract Like in other vertebrates, the anterior part of the telencephalon of amphibians mainly consists of the olfactory bulb (OB), but different from higher vertebrates, the lateral telencephalic ventricles of larval *Xenopus laevis* expand deep into the anterior telencephalon. The neurogenic periventricular zone (PVZ) of the lateral ventricles generates new OB neurons throughout the animal's lifetime. We investigated the ultrastructural organization of the PVZ and found that within a time period of 24 h, 42.54± 6.65% of all PVZ cells were actively proliferating. Functional purinergic receptors are widespread in the central nervous system and their activation has been associated with many critical physiological processes, including the regulation of cell proliferation. In the present study we identified and characterized the purinergic system of the OB and the PVZ. ATP and 2MeSATP induced strong $[Ca^{2+}]_i$ increases in cells of both regions, which could be attenuated by purinergic antagonists. However, a more thorough pharmacological investigation revealed clear differences between the two brain regions. Cells of the OB almost exclusively express ionotropic P2X purinergic receptor subtypes, whereas PVZ cells express both ionotropic P2X and metabotropic P1 and P2Y receptor subtypes. The P2X receptors expressed in the OB are evidently not involved in the immediate processing of olfactory information.

Keywords P1 receptors · P2 receptors · Olfaction · Neuronal stem cells · Subventricular zone

T. Hassenklöver · P. Schulz · A. Peters · D. Schild · I. Manzini (✉)
Department of Neurophysiology and Cellular Biophysics,
University of Göttingen,
Humboldtallee 23,
37073 Göttingen, Germany
e-mail: imanzin@gwdg.de

T. Hassenklöver · D. Schild · I. Manzini
DFG Research Center for Molecular Physiology of the Brain (CMPB), University of Göttingen,
Humboldtallee 23,
37073 Göttingen, Germany

P. Schwartz
Department of Anatomy and Embryology, Center of Anatomy,
University of Göttingen,
Kreuzbergring 36,
37075 Göttingen, Germany

D. Schild
DFG Cluster of Excellence 171,
Humboldtallee 23,
37073 Göttingen, Germany

Introduction

The anterior part of the telencephalon of larval *Xenopus laevis* is primarily involved in the processing of olfactory information. It mainly consists of the olfactory bulb (OB), the first relay center of the olfactory system. This structure processes chemosensory stimuli detected in the peripheral olfactory organs and transfers this information to higher brain centers [1]. The basic organization of the OB is highly conserved across phyla [2]. From the surface to the center, the OB can be subdivided in six discernible layers: the nerve layer, the glomerular layer, the external plexiform layer, the mitral cell layer, the internal plexiform layer and the granule cell layer. The most caudal layer, the granule cell layer, contacts the lateral telencephalic ventricles, which in larval *X. laevis* expand deep into the anterior telencephalon [3]. The area surrounding the lateral ventricles, the so-called periventricular zone (PVZ), has been

reported to be a neurogenic region comprising neuronal stem cells [4]. Recent studies have shown that the proliferating cells of the PVZ of the lateral ventricles in larval and adult *X. laevis* are homologous to neural stem cells of higher vertebrates [3]. In mammals, the cells of the embryonic and adult PVZ of many brain regions have been thoroughly characterized [5–8]. In lower vertebrates such as amphibians, comparable detailed studies are lacking.

Extracellular nucleotides act via purinergic receptors, which have been divided in two main families: adenosine or P1 receptors and P2 receptors [9]. The P1 receptors all couple to G proteins and have been further subdivided into four subtypes (A_1, A_{2A}, A_{2B}, and A_3). The P2 receptors have been split into ionotropic P2X receptors and G protein coupled P2Y receptors. To date, seven subtypes of P2X receptors ($P2X_1$–$P2X_7$) and eight subtypes of P2Y receptors ($P2Y_1$, $P2Y_2$, $P2Y_4$, $P2Y_6$, $P2Y_{11}$, $P2Y_{12}$, $P2Y_{13}$, and $P2Y_{14}$) have been described [10–12]. An additional P2Y receptor, named $P2Y_8$, with an extremely broad agonist selectivity has been cloned from *X. laevis* embryos [13]. Activation of purinergic receptors has been shown to play an important role in many physiological processes [14], including embryonic and adult neurogenesis [14, 15] and neuron–glia interactions in the OB [16]. It has been shown, mainly by means of immunohistochemical studies, that purinergic receptors and associated nucleotide-degrading enzymes are expressed in the murine OB and PVZ [14, 15]. However, a thorough functional study of the purinergic system of these two brain regions is as yet missing, and to our knowledge in non-mammalian vertebrates there are no studies at all.

In the present study, we described the ultrastructural organization of the PVZ of larval *X. laevis*, and determined the proliferation rates of its neuronal stem cells. We then identified and investigated the purinergic system of the OB and its neurogenic PVZ and demonstrate that activation of purinergic receptors initiates stereotypic Ca^{2+} signaling in cells of both brain areas. Thereby, we found that cells of the two brain areas express different purinergic receptor subtypes. Also, we obtained evidence that the purinergic receptors expressed in the OB are not evidently involved in the immediate processing of olfactory information. Possible physiological roles of the purinergic system in the OB and the PVZ are discussed.

Materials and methods

Slices of the anterior telencephalon and nose–brain preparations

Larval *X. laevis* (stages 51 to 54; staged after [17]) were cooled to produce complete immobility, and then killed by transection of the brain at its transition to the spinal cord. All procedures for animal handling and tissue dissections were carried out according to the guidelines of the Göttingen University Committee for Ethics in Animal Experimentation. For slices of the anterior telencephalon, a block of tissue containing the terminal part of the olfactory nerves and the anterior brain was cut out. Then, the tissue was glued onto the stage of a vibroslicer (VT 1000S, Leica, Bensheim, Germany), cut horizontally into one 120–130 μm thick slice and kept in bath solution. For nose–brain preparations a block of tissue containing the olfactory epithelia, the olfactory nerves and the anterior part of the brain was cut out and kept in bath solution. The tissue was then glued onto the stage of the vibroslicer and only the dorsal surface of the OB was sliced off. The olfactory epithelia were left intact. For a more detailed description of these preparations see earlier work of our lab [18, 19] and Figs. 3 and 8.

Solutions, staining protocol, and stimulus application

Standard bath solution consisted of (in mM): 98 NaCl, 2 KCl, 1 $CaCl_2$, 2 $MgCl_2$, 5 glucose, 5 Na-pyruvate, 10 HEPES, 230 mOsmol/l, pH 7.8. Ca^{2+}-free bath solution consisted of (in mM): 98 NaCl, 2 KCl, 2 $MgCl_2$, 5 glucose, 5 Na-pyruvate, 10 HEPES, 2 EGTA, 230 mOsmol/l, pH 7.8.

Tissue preparations were transferred to a recording chamber, and bath solution containing 50 μM Fura-2/AM (Molecular Probes, Leiden, The Netherlands) was added. Fura-2/AM was dissolved in DMSO (Sigma, Deisenhofen, Germany) and Pluronic F-127 (Molecular Probes). The final concentrations of DMSO and Pluronic F-127 did not exceed 0.5% and 0.1%, respectively. Cells of the nervous system of larval *X. laevis* express multidrug transporters [20, 21] with a wide substrate spectrum, including calcium-indicator dyes. To avoid transporter-mediated destaining of the slices, 50 μM MK571 (Alexis Biochemicals, Grünberg, Germany), an inhibitor of multidrug transporters was added to the incubation solution. The preparations were incubated on a shaker at room temperature for 35 min.

5-Bromo-2′-deoxyuridine (BrdU); adenosine; adenosine-5′-diphosphate (ADP); adenosine-5′-triphosphate (ATP); uridine; uridine-5′-triphosphate (UTP); α,β-methylene-ATP (α,β-MeATP); β,γ-methylene-ATP (β,γ-MeATP); 2-methylthio-ATP (2MeSATP); 3′-*O*-(4-benzoyl)benzoyl ATP (BzATP); suramin, pyridoxalphosphate-6-azophenyl-2′,4′-disulfonic acid (PPADS), 6-cyano-7-nitroquinoxaline-2,3-dione (CNQX), D(−)-2-amino-5-phosphonopentanoic acid (APV) and bath solution chemicals were purchased from Sigma.

As odorants, we used a mixture of 15 L-amino acids (glycine, alanine, serine, threonine, cysteine, valine, leucine, isoleucine, methionine, proline, arginine, lysine, histidine, phenylalanine, and tryptophan, all from Sigma, each at a concentration of 100 μM).

Bath solution was applied by gravity feed from a storage syringe through a funnel drug applicator to the recording chamber. In the experiments with slices of the anterior telencephalon, the purinergic agonists were pipetted directly into the funnel (placed above the anterior telencephalon) without stopping the flow. In all experiments with the nose–brain preparation, odorants were pipetted directly into the funnel drug applicator placed above the intact olfactory epithelium. An additional bath solution applicator for application of purinergic agonists and antagonists was positioned above the OB (see Fig. 8). Outflow was through a syringe needle placed at the height of the olfactory nerves in both preparations.

Ca^{2+} imaging and data evaluation

For calcium imaging, Fura-2-stained preparations were fixed with a grid in a recording chamber and placed on the stage of an upright microscope (Axioskop 2, Zeiss, Göttingen, Germany). Fluorescence images (excitation at 380 nm; emission >505 nm) were recorded using a frame-transfer, back-illuminated CCD camera (16 bits/pixel, Micromax; Visitron, München, Germany) and a custom-built monochromator. With this configuration intracellular calcium concentration $[Ca^{2+}]_i$ increases are accompanied by a decrease of the Ca^{2+}-dependent fluorescence. Images were acquired at 200 to 500 ms exposure time per image using the commercial image acquisition software Winview (Visitron). Before starting the imaging experiments, the slices were rinsed with bath solution for at least 5 min.

Image analysis was performed using custom programs written in MATLAB (MathWorks, Natick, USA). To facilitate selection of regions of interest, a "pixel correlation map" was obtained by calculating the cross-correlation between the fluorescence signals of a pixel to that of its immediate neighbors and then the resulting values were displayed as a grayscale map. The fluorescence changes for individual regions of interest are given as $\Delta F/F$ values. For more detailed information see our previous work [22]. Because some slices showed a linear loss of fluorescence intensity over time (bleaching artifacts) the $\Delta F/F$ values used to present all averaged data, presented as mean ± SEM (standard error of the mean), were corrected to retain comparability. On the basis of the first ten and the last four data points of each recording a linear fitting was calculated using MATLAB functions and subtracted from the raw data. For the calculation of the proliferation rate, series of brain slices (70 μm thickness, two to four slices per animal) were prepared, and multiple fields of view were visualized to include the whole PVZ of both sides. Cell nuclei labeled with propidium iodide and BrdU were counted automatically using CellProfiler [23]. Counting results were verified by inspecting overlays of automatically identified objects on the original images.

BrdU injections and histology

To stain cells in the S phase of their cell cycle, larval *X. laevis* (stages 51 to 54) were anesthetized, and 200 μM BrdU, a synthetic nucleoside that is an analogue of thymidine [24], was injected intraperitoneally. After 16–18 h additional 200 μM BrdU were injected to sustain high BrdU levels. After 24 h the animals were sacrificed and a tissue block containing the anterior part of the brain was removed. For BrdU-immunohistochemistry, the removed tissue blocks were fixed in 4% formaldehyde, washed in phosphate buffer saline (PBS), embedded in 5% low melting point agarose (Sigma) and sectioned on the vibratome at 70 μm. Sections were washed in PBS containing 0.2% Triton X-100 (PBST), and non-specific binding was blocked with 2% normal goat serum (NGS; ICN, Aurora, Ohio, USA) in PBST for 1 h at room temperature. The slices were then incubated in 1 N HCl at 37°C for 45 min to denature DNA. Subsequently, the slices were incubated overnight at 4°C with primary antibodies [anti BrdU (B2531, monoclonal, derived from mouse, Sigma) diluted in 2% NGS/PBST (1:1,000)]. The primary antibodies were washed off with PBS and Alexa 488 conjugated goat anti mouse secondary antibodies (Molecular Probes) were applied at a dilution of 1:250 in 1% NGS/PBS for 2 h at room temperature. The secondary antibodies were washed off in several changes of PBS. Cell nuclei were stained with propidium iodide.

For purinergic receptor immunohistochemistry, formaldehyde fixed brains were washed in PBS, embedded in 5% low melting point agarose (Sigma), and subsequently sectioned on the vibratome at 70 μm. Sections were then washed in PBST, and non-specific binding was blocked with 2% NGS in PBST for 1 h at room temperature. Tissue was then incubated overnight at 4°C with the primary antibodies [anti rat $P2X_1$, anti rat $P2X_2$, anti rat $P2X_4$, anti rat $P2X_7$, anti rat $P2Y_2$, and anti rat $P2Y_4$ (1:200, raised in rabbit, Alomone Labs, Jerusalem, Israel] diluted in 2% NGS/PBST. Primary antibodies were washed off with PBS, and Alexa 488 conjugated goat anti rabbit secondary antibodies (Molecular Probes) were applied at a dilution of 1:250 in 1% NGS/PBS for 2 h at room temperature. The secondary antibody was washed off in several changes of PBS. The specificity of the anti P2 receptor antibodies used was previously assessed by the producer and evaluated in *X. laevis* by incubating slices with the anti P2 antibodies (1:200) preadsorbed, 1 h at room temperature, with the immunizing peptide provided by the producer.

Slices were then transferred to slides and mounted in mounting medium (Daco, Hamburg, Germany). Images were acquired with a confocal laser-scanning microscope (Zeiss LSM 510/Axiovert 100 M, Jena, Germany).

For transmission electron microscopy, specimens were fixed with 1.5% glutaraldehyde and 1.5% paraformaldehyde in 0.1 M sodium phosphate buffer, pH 7.3 for 3 h at room temperature and then postfixed for 2 h in 2% osmium tetroxide in 0.1 M sodium phosphate buffer. Samples were embedded in Araldite after dehydration in graded ethanol. To obtain a general overview of the samples semithin sections (1 μm) were cut with an Ultracut E (Leica), mounted on micro slides and stained with Methylenblue-Azur II for 1 min and viewed under an Axioplan 2 (Zeiss, Oberkochen, Germany) to which an Axiocam MRc 5 (Zeiss) was attached. Ultrathin sections were cut with an Ultracut E (Leica), mounted on copper grids, poststained with uranyl acetate and lead citrate and viewed under a LEO 900 (Zeiss).

Results

Description of the neurogenic PVZ of the anterior telencephalon

A general overview of the telencephalon of larval *X. laevis* is given in Fig. 1a. To investigate the ultrastructural organization of the cell layers surrounding the lateral telencephalic ventricles we performed transmission electron microscopy. Figure 1b (b_1) shows the anterior part of the lateral telencephalic ventricle, the PVZ and the posterior part of the granule cell layer of the OB. The transition between the anterior PVZ, adjacent to the OB, and the granule cell layer can be clearly identified (dotted line). Generally, the cells within the PVZ appear more electron dense than those in the adjacent cells layers. The neuronal stem-/progenitor cells within the anterior PVZ are arranged in four to five cell layers with irregular or oval nuclei that present, in some cases, small invaginations and prominent nucleoli (Fig. 1b, b_2). Thereby, the cells contacting the ventricular lumen do not apparently differ from those within the other cell layers and are devoid of cilia or microvilli. The asterisk shows a neuronal stem-/progenitor cell in mitosis. Highly condensed DNA (chromosomes) is clearly visible showing that cells in the PVZ proliferate. The cell bodies of the granule cells have a more regular, roundish shape. The medial PVZ is made of about three to four cell layers and its cells basically resemble those of the anterior PVZ (Fig. 1b, b_3). Some of them also have prominent nucleoli and they feature chromatin in different states of aggregation, probably representing pre- or post-mitotic stages of the cell cycle. As in the anterior part of the PVZ, also here the cells in direct contact with the lateral ventricle do not bear cilia or microvilli. The PVZ situated laterally to the ventricle appears thinner than in the anterior and medial part (Fig. 1b, b_4). It is composed of more tightly packed cells arranged in at most two cell layers. Most cells have elongated nuclei and are devoid of cilia or microvilli. Figure 1b (b_5 and b_6) depicts higher magnification images of PVZ cells, two of them in mitosis, contacting the lumen of the lateral ventricle. The luminal parts of the cells are tightly packed with mitochondria. One cell exhibits a large cytoplasmic protrusion into the lumen of the ventricle; another cell exhibits a multivesicular protrusion expanding into the ventricle. This image shows also one of the rare cells extending a single cilium into the cerebrospinal fluid.

To determine the proliferation rate of the PVZ cells and to further define the border between the neurogenic PVZ and the adjacent OB, we combined propidium iodide cell nuclei staining and a BrdU incorporation assay. In the adopted survey time window (see the "Materials and methods" section) the BrdU-positive cells, i.e., the proliferating cells, were confined to the PVZ. This helped to determine the approximate borders between the two brain regions (Fig. 2). Thereby, we found that the proliferation rate of PVZ cells is rather high. 42.54±6.65% (SEM; n=3 animals, 6 OBs/PVZs) of all cells surrounding the lateral ventricles were BrdU-positive.

Nucleotide-induced increases of $[Ca^{2+}]_i$ in cells of the anterior telencephalon

Figure 3a (a_1–a_3) show a larva of *X. laevis*, a slice preparation of its telencephalon and a slice of the anterior part of the telencephalon stained with the fluorescent calcium-indicator dye Fura-2, respectively. To visualize nucleotide-induced $[Ca^{2+}]_i$ signals in cells of the anterior telencephalon, we performed calcium imaging experiments. Figure 3b (b_1) shows the same slice as in Fig. 3a (a_3), with the red-shaded area covering the OB and the green shaded area covering the PVZ. Application of 5 μM 2MeSATP led to specific transient cellular response patterns in the vast majority of cells (Fig. 3b, b_2). The response time courses of six individual cells of the OB and six cells of the PVZ are plotted in Fig. 3b (b_3–b_4). Figure 3b (b_5) shows the mean (±SEM) intracellular Ca^{2+} transients of all 2MeSATP-responsive cells of this OB and PVZ. Application of ATP (50 μM) to the same slice preparation elicited similar, though smaller $[Ca^{2+}]_i$ transients (Fig. 3b, b_6). Similar results were obtained in more than 20 slices of the anterior telencephalon tested for their responsiveness to 2MeSATP and ATP. These results strongly suggest that both, OB cells and PVZ cells, are endowed with purinergic receptors. To exclude purinergic receptor desensitization, interstimulus intervals of at least 5 min were chosen in all of the experiments. Fig. 3c shows that ATP-induced $[Ca^{2+}]_i$ increases remain stable using this experimental protocol.

To confirm that the nucleotide-induced responses were truly mediated by purinergic receptors, we tested the effects of two acknowledged P2 receptor antagonists. In both brain regions, the OB and the PVZ, 2MeSATP- and ATP-induced

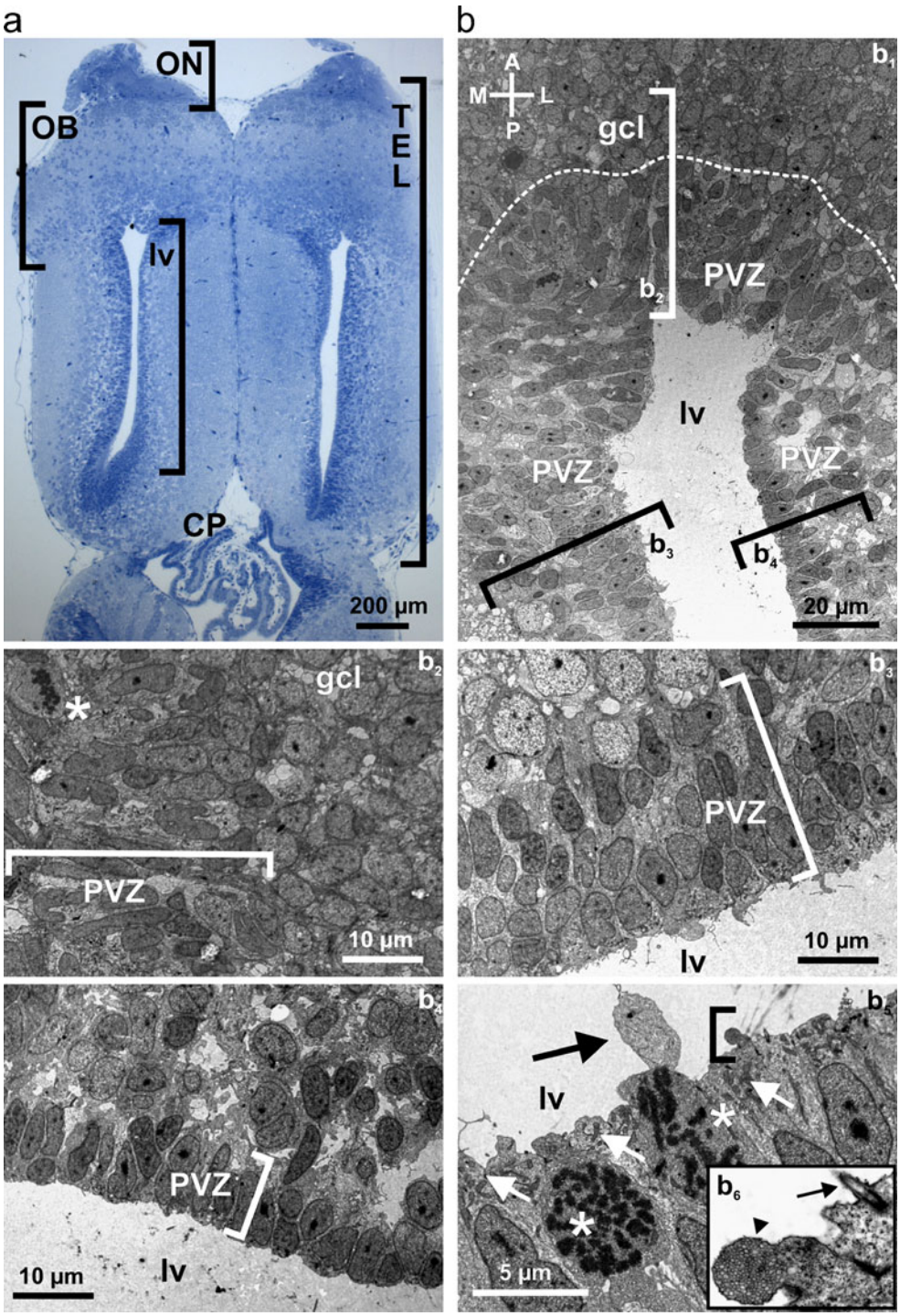

Fig. 1 Ultrastructural analysis of the anterior telencephalon. **a** Horizontal slice of the telencephalon of larval *X. laevis* stained with Methylenblue-Azur II. **b** Transmission electron microscopy of the anterior part of the lateral telencephalic ventricles with its PVZ and the posterior part of the granule cell layer of the OB (b_1). Various electron micrographs were assembled into a photo montage to obtain this overview. The *dotted line* indicates the approximate border between the PVZ and the granule cell layer of the OB. The *brackets* indicate the approximate location of the areas shown at higher magnification in b_2 through b_4. Anterior part of the PVZ and adjacent granule cell layer of the OB (b_2). Cell divisions are frequent in the PVZ. Note the cell with decomposed nuclear envelope and condensed DNA in form of chromosomes (*asterisk*). Medial part of the PVZ (b_3) and lateral part of the PVZ (b_4). The *brackets in* b_2 *through* b_4 include the cell layers of the anterior, medial, and lateral PVZ, respectively. b_5 shows a higher magnification of cells in direct contact with the lumen of the lateral ventricles. Two cells are in mitosis (*asterisks*). The *white arrows* indicate accumulations of mitochondria very close to the ventricular lumen. The *black arrow* shows a large cellular protrusion into the ventricle. The area included in the bracket is shown at higher magnification in b_6. Note the multivesicular protrusion into the ventricle (*arrowhead*) and the single cilium extending into the cerebrospinal fluid (*arrow*). Abbreviations: *ON* olfactory nerve, *OB* olfactory bulb, *PVZ* periventricular zone, *TEL* telencephalon, *CP* choroid plexus, *lv* lateral ventricle, *gcl* granule cell layer

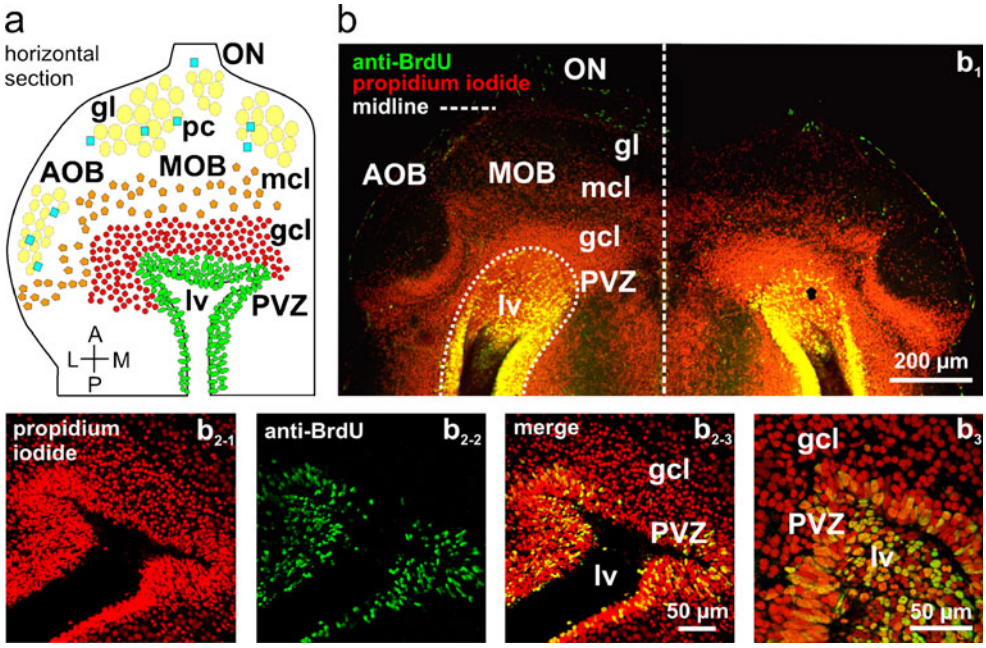

Fig. 2 Cells in the periventricular zone of the lateral ventricle actively proliferate. **a** Schematic representation of the anterior telencephalon of larval *X. laevis*. **b** Overview over a horizontal section of the anterior telencephalon (b_1) in which all cell nuclei were stained with propidium iodide (*red fluorescence*) and proliferating cells were visualized with a BrdU incorporation assay (*green fluorescence*). Proliferating cells appear yellow. Higher magnification of the periventricular region of different animals ($b_{2\text{-}1}$–$b_{2\text{-}3}$ and b_3). Abbreviations: *ON* olfactory nerve, *MOB* main olfactory bulb, *AOB* accessory olfactory bulb, *PVZ* periventricular zone, *gl* glomerular layer/glomeruli, *mcl* mitral cell layer, *gcl* granule cell layer, *lv* lateral ventricle, *pc* periglomerular cells

$[Ca^{2+}]_i$ increases were reduced in presence of suramin (200 µM; Fig. 4a and b) and PPADS (200 µM; Fig. 4c and d). Nevertheless, the observed effect of suramin on 2MeSATP-induced responses in both brain regions and on ATP-induced responses in the PVZ was not statistically significant. It has been shown that glutamate mediates most or all excitatory synaptic interactions between OB cells via ionotropic receptors [1, 25], and extracellular nucleotides acting on purinergic receptors have been shown to be able to induce glutamate release from neuronal [26, 27] and glial cells [26, 28, 29]. To exclude a contribution of ionotropic glutamate receptors in the $[Ca^{2+}]_i$ increases recorded in cells of the anterior telencephalon, we tested the effect of the AMPA and NMDA receptor antagonist CNQX and APV. Figure 4e and f show that the ATP-induced peak responses remained virtually unchanged in both regions when the ionotropic glutamate receptors were blocked.

To test whether metabotropic and/or ionotropic purinergic receptors are expressed in the OB and the PVZ, we performed experiments with Ca^{2+}-free extracellular bath solution. Although in both brain regions, 2MeSATP- and ATP-induced $[Ca^{2+}]_i$ increases were significantly reduced in Ca^{2+}-free bath solution, the reduction was consistently greater in the OB (Fig. 5). PVZ cells of all slices tested clearly retained some residual responses. After returning to standard bath solution, the responses recovered almost completely. This set of data unambiguously shows that OB cells are endowed almost exclusively with ionotropic P2X receptor(s), while PVZ cells in addition to an important fraction of ionotropic P2X receptors most likely express also some metabotropic purinergic receptors.

To substantiate the above results and to obtain an indication of which purinergic receptor subtypes are expressed in the OB and the PVZ, we examined the potency of nine purinergic agonists known to differentially activate purinergic receptor subtypes, and compared their efficacy to elicit $[Ca^{2+}]_i$ increases in cells of these brain regions. The obtained results are shown in Fig. 6. Thereby, the most evident differences were observed with adenosine and ADP. While these two agonists were almost ineffective in the OB, they induced clear $[Ca^{2+}]_i$ increases in cells of the PVZ. Also ATP induced significantly stronger responses in cells of the PVZ, but in contrast to adenosine and ADP, it induced clear responses also in the OB. 2MeSATP and BzATP elicited strong $[Ca^{2+}]_i$ increases in cells of both regions. While 2MeSATP was almost equipotent in the OB and the PVZ, BzATP was more effective in the OB. α,β-MeATP, β,γ-MeATP, uridine and UTP were inactive or very weakly active in both regions.

Immunohistochemical localization of purinergic receptors

To gain additional information about the purinergic receptor subtypes expressed in the anterior telencephalon, we

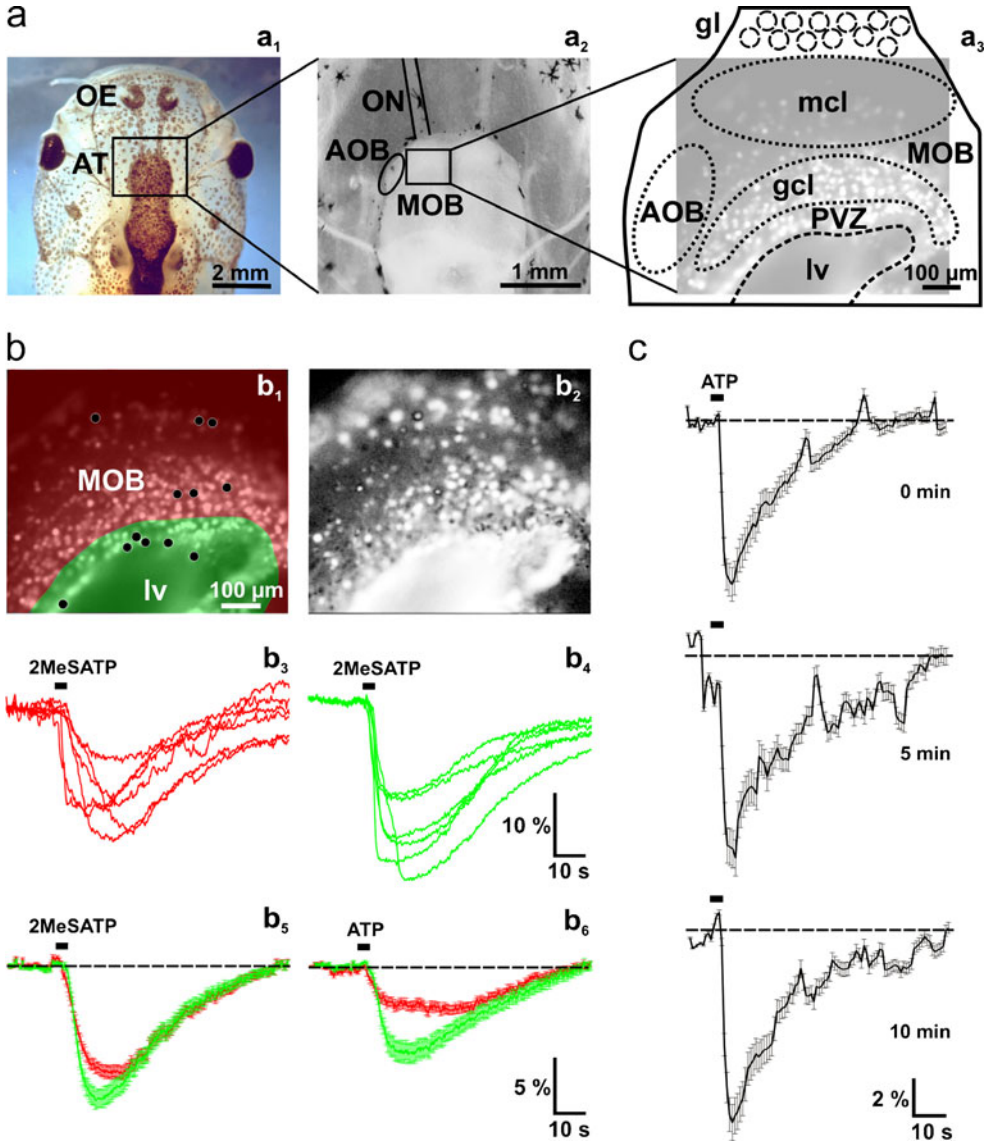

Fig. 3 Nucleotide-induced $[Ca^{2+}]_i$ increases in cells of the anterior telencephalon. **a** Overview of a head of larval *X. laevis* (a_1). The *black rectangle* indicates the location of the anterior telencephalon. An acute slice preparation of the telencephalon is shown in a_2. The black rectangle indicates the approximate location of the Fura-2/AM stained slice shown in a_3 (*brightened fluorescence image acquired at rest*). **b** Fura-2/AM stained slice preparation (the same as shown in a_3) with the area of the OB shaded in *red*, and the PVZ shaded in *green* (b_1). Pixel correlation map of the same slice (see "Materials and methods" section for details) obtained upon application of 2MeSATP (5 µM; b_2). The ventricle appears to respond as a whole. This results from responses of ependymal cells from the floor of the lateral ventricle. The 2MeSATP-induced $[Ca^{2+}]_i$ transients of six individual cells of the OB (see *black dots in the red-shaded area* in b_1) and the PVZ (see *black dots in the green shaded area* in b_1) are shown in b_3 and b_4, respectively. The 2MeSATP-induced mean $[Ca^{2+}]_i$ transients (±SEM) of all clearly identifiable responsive cells of the OB (*red traces*; n=138) and the cells of the PVZ (*green traces*; n=32) of this slice are shown in b_5. Application of ATP (50 µM) to the same slice preparation induced comparable $[Ca^{2+}]_i$ transients in the same cells as above (b_6). (**c**) Mean $[Ca^{2+}]_i$ transients of responding OB and PVZ cells (n=120) remain stable after repeated applications of ATP (100 µM; interstimulus interval: 5 min). Abbreviations: *OE* olfactory epithelium, *AT* anterior telencephalon, *ON* olfactory nerve, *MOB* main olfactory bulb, *AOB* accessory olfactory bulb, *PVZ* periventricular zone, *gl* glomerular layer/glomeruli, *mcl* mitral cell layer, *gcl* granule cell layer, *lv* lateral ventricle

employed antibody stainings. We obtained positive results with antibodies against $P2X_7$ and the $P2X_4$ subtypes. Preincubation with the immunizing peptide specifically blocked the staining. $P2X_7$- and $P2X_4$-like immunoreactivity was found on cells of both the OB and the PVZ. Antibodies against the $P2X_7$ receptor subtype showed a somatic staining pattern in cells of both the OB and the PVZ (Fig. 7a). Antibodies against the $P2X_4$ receptor subtype showed a clear somatic staining pattern in OB cells (Fig. 7b, b_1). Interestingly, higher magnification pictures of the PVZ revealed a positive $P2X_4$-like staining of tubular structures starting from the ependymal layer of the lateral ventricle and extending

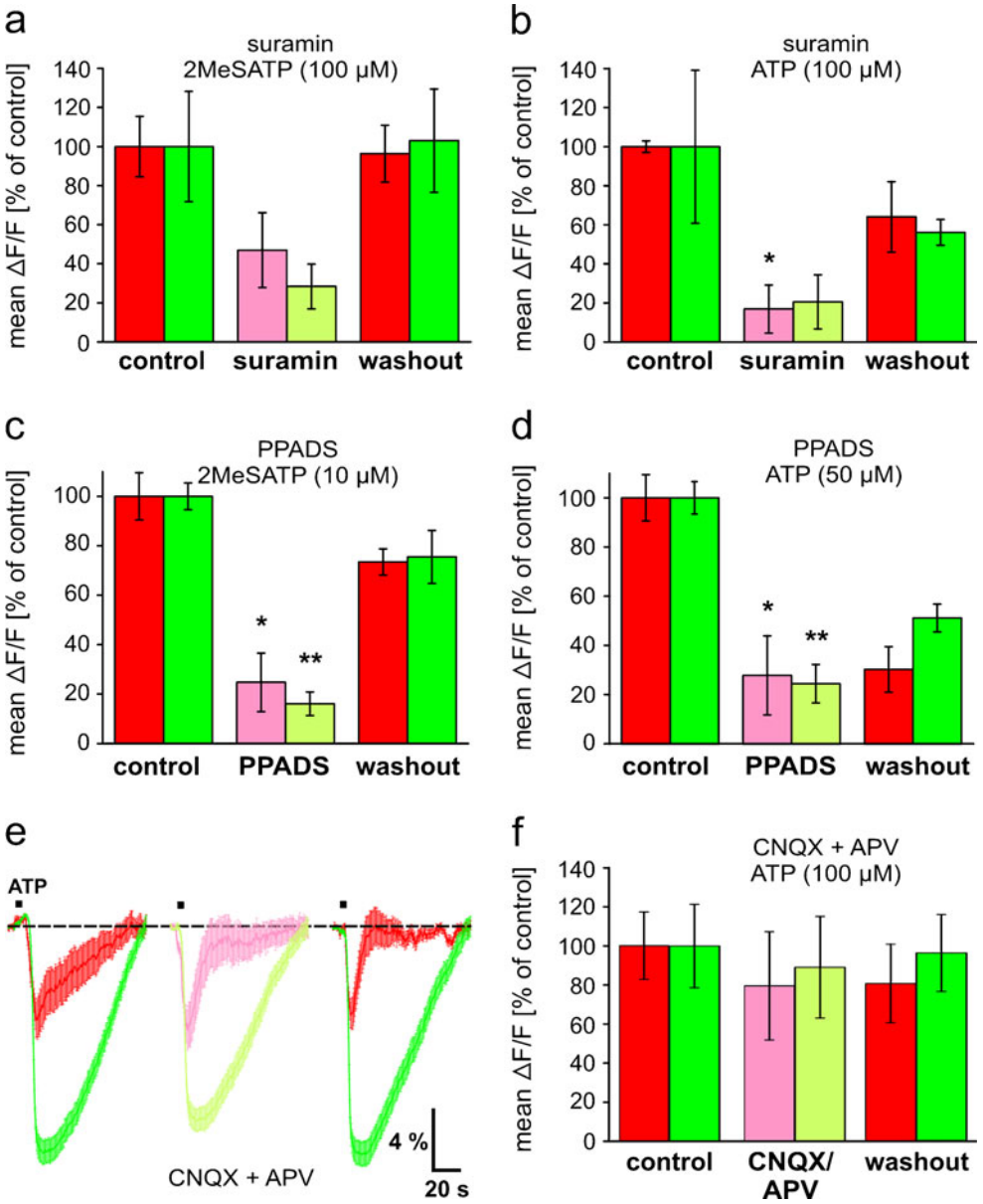

Fig. 4 Effects of purinergic and glutamatergic antagonists on nucleotide-induced $[Ca^{2+}]_i$ increases in cells of the anterior telencephalon. **a** Mean peak responses (±SEM), expressed as percent of control response to 2MeSATP (100 µM), of 186 OB cells and 80 PVZ cells (three slices of the anterior telencephalon) in control conditions (*red and green columns on the left-hand side*, respectively), after 10 min in bath solution with 200 µM suramin (*light red and light green column*, respectively), and after 10 min of washout with bath solution (*red and green columns on the right-hand side*, respectively). **b** Same representation as in **a** with ATP (100 µM) and suramin [200 µM; 90 OB cells and 72 PVZ cells (two and three slices of the anterior telencephalon, respectively)]. **c** Same representation as in **a** with 2MeSATP (10 µM) and PPADS [200 µM; 155 OB cells and 216 PVZ cells (two slices of the anterior telencephalon)]. **d** Same representation as in **a** with ATP (50 µM) and PPADS [200 µM; 242 OB cells and 262 PVZ cells (three slices of the anterior telencephalon)]. **e** The peak amplitudes of ATP-induced (100 µM) mean $[Ca^{2+}]_i$ transients (±SEM) of all responsive cells (OB: n=21, *red traces*; PVZ: n=47, *green traces*) of an individual slice of the anterior telencephalon are not significantly attenuated by 50 µM CNQX and 200 µM APV (OB: *light red trace*; PVZ: *light green trace*). **f** Mean peak responses (±SEM), expressed as percent of control response to ATP (100 µM), of 287 OB cells and 360 PVZ cells (seven slices of the anterior telencephalon) in control conditions (*red and green columns on the left-hand side*, respectively), after 5 min in bath solution with 50 µM CNQX and 200 µM APV (*light red and light green column*, respectively), and after 10 min of washout with bath solution (*red and green columns on the right-hand side*, respectively). (*p<0.05 and **p<0.01; unpaired t test)

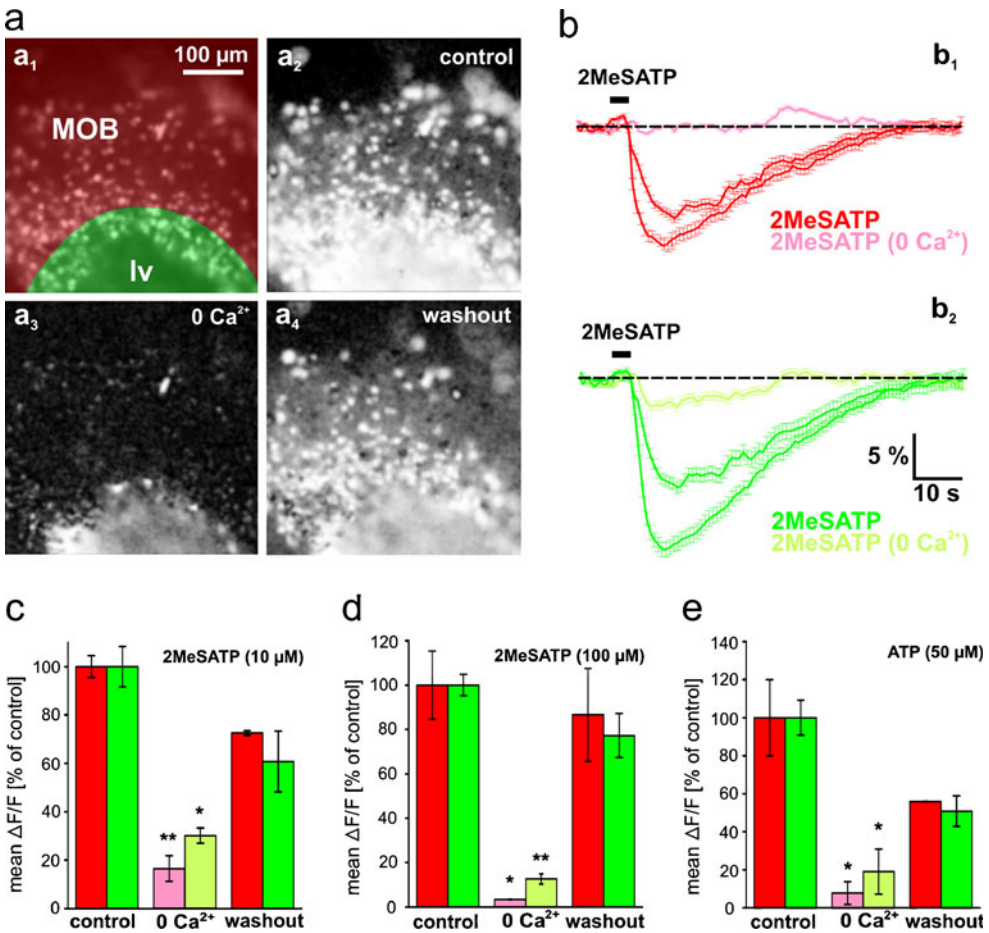

Fig. 5 Nucleotide-induced responses of OB and PVZ cells are differentially affected by omission of extracellular Ca^{2+}. **a** Fura-2/AM stained acute slice preparation of the anterior telencephalon (a_1; image acquired at rest). The area of the OB is *shaded in red*, and the area of the PVZ is *shaded in green*. Pixel correlation maps of the same slice (see "Materials and methods" section for details) obtained upon application of 2MeSATP (100 µM; a_2 standard bath solution; a_3 application after 10 min in Ca^{2+}-free bath solution; a_4 application after returning to standard bath solution). **b** The corresponding 2MeSATP-induced mean $[Ca^{2+}]_i$ transients (±SEM) of all clearly identifiable responsive cells of the OB [b_1 *red traces*: in normal bath solution (before and after application of Ca^{2+}-free bath solution); *light red traces*: after 10 min in Ca^{2+}-free bath solution; $n=82$ cells] and of the PVZ [b_2 *green traces*: in normal bath solution (before and after application of Ca^{2+}-free bath solution); *light green traces*: after 10 min in Ca^{2+}-free bath solution; $n=59$ cells]. **c** Mean peak responses (±SEM), expressed as percent of control response to 2MeSATP (10 µM), of 161 OB cells and 182 PVZ cells (two slices of the anterior telencephalon) in control conditions (*red and green columns*, respectively) and after 10 min in Ca^{2+}-free bath solution (*light red and light green column*, respectively). **d** Same representation as in C with 2MeSATP [100 µM; 205 OB cells and 105 PVZ cells (two slices of the anterior telencephalon)]. **e** Same representation as in C with ATP [50 µM; 161 OB cells and 182 PVZ cells (two slices of the anterior telencephalon)]. (*$p<0.05$ and **$p<0.01$; unpaired t test). Abbreviations: *MOB* main olfactory bulb, *lv* lateral ventricle

into the OB (Fig. 7b, b_2). No staining was observed with antibodies against $P2X_1$, $P2X_2$, $P2Y_2$, and $P2Y_4$ receptor subtypes (data not shown).

Influence of the telencephalic purinergic system on the processing of olfactory information

As a last point, we investigated the possibility of a direct purinergic modulation of odorant information processing in the OB network. These experiments were performed using a nose–brain preparation (see Fig. 8a), and amino acids as olfactory stimuli. The nose–brain preparation allows to stimulate the olfactory epithelium with odorants and to simultaneously monitor the odorant-induced responses in the OB.

Continuous stimulation of the OB with purinergic agonists (2MeSATP or ATP) or the P2 receptor antagonist suramin did not disrupt the odorant-induced responses of OB cells. Figure 8b shows the mean (±SEM) intracellular amino acid-induced $[Ca^{2+}]_i$ transients of all responsive OB cells (b_1; upper row) and the amino acid-induced $[Ca^{2+}]_i$ transient of a randomly chosen individual cell of the same slice (b_1; lower row). The overall appearance of the responses did not notably change after OB perfusion with 2MeSATP (gray-shaded area). Similarly, also prolonged application of ATP or suramin did not notably change the mean (±SEM) amino acid-induced

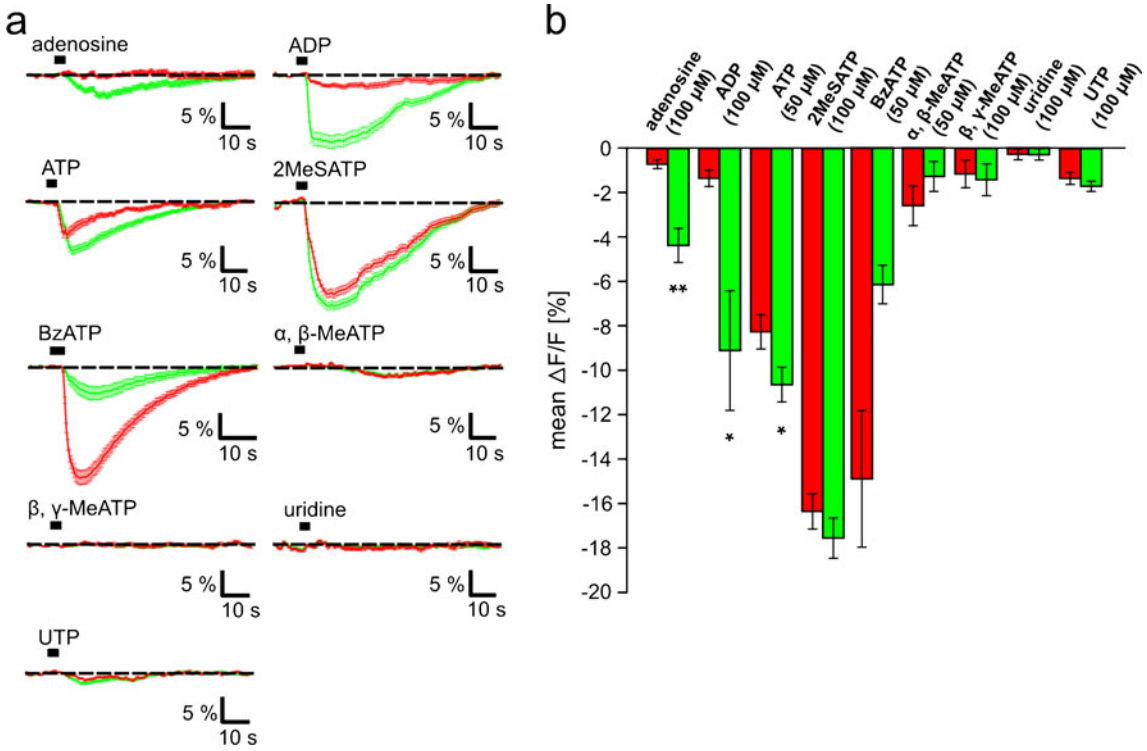

Fig. 6 Responsiveness of OB and PVZ cells to purinergic receptor agonists. **a** Mean $[Ca^{2+}]_i$ transients (±SEM) of all clearly identifiable responsive cells of an OB (*red traces*) and a PVZ (*green traces*). Traces originate from more than one tissue slice. **b** The mean peak amplitude of agonist-induced responses (±SEM) of cells of the OB and the PVZ were compared (*red columns* OB cells, green columns *PVZ cells*). [adenosine (100 μM), data from 170 OB cells and 236 PVZ cells from 6 slices of the anterior telencephalon; ADP (100 μM), 245 OB cells and 154 PVZ cells from three slices; ATP (50 μM), 1566 OB cells and 1303 PVZ cells from 28 and 23 slices, respectively; 2MeSATP (100 μM), 378 OB cells and 285 PVZ cells from five slices; BzATP (50 μM), 213 OB cells and 93 PVZ cells from four and two slices, respectively; α,β-MeATP (50 μM), 310 OB cells and 198 PVZ cells from six and three slices, respectively; β,γ-MeATP (100 μM), 387 OB cells and 318 PVZ cells from seven and six slices, respectively; uridine (100 μM), 275 OB cells and 308 PVZ cells from six slices; UTP (100 μM), 335 OB cells and 324 PVZ cells from five slices]. (*$p<0.05$ and **$p<0.01$; unpaired *t* test). Abbreviations: *ADP* adenosine-5′-diphosphate, *ATP* adenosine-5′-triphosphate, *UTP* uridine-5′-triphosphate; *α,β-MeATP* α,β-methylene-ATP, *β,γ-MeATP* β,γ-methylene-ATP, *2MeSATP* 2-methylthio-ATP, *BzATP*, 3′-*O*-(4-benzoyl)benzoyl ATP

$[Ca^{2+}]_i$ transients of OB cells (Fig. 8b, b_2 and b_3). Figure 8c (c_1–c_3) summarizes the results obtained from all amino acid-responding OB cells from various nose–brain preparations treated with 2MeSATP, ATP and suramin, respectively.

Discussion

The purinergic system employs extracellular purines and pyrimidines as signaling molecules [9]. In the nervous system, both neurons as well as glial cells have been shown to express various subtypes of purinergic receptors [14]. The purinergic receptors of many brain regions have been thoroughly characterized, and the effects of their activation intensively studied [14, 30]. However, the information available about the purinergic system of the OB and the neurogenic PVZ is rather limited. There is evidence for P1 receptors [16], P2X receptors ($P2X_2$: [31–33]; $P2X_4$: [34–36]; $P2X_5$: [37]; $P2X_6$: [35, 38]; $P2X_7$: [39]) and P2Y receptors ($P2Y_1$: [40]; $P2Y_2$: [33]) in the murine OB and for P2X receptors ($P2X_{1\text{-}6}$: [41]; $P2X_2$: [32]; $P2X_6$: [35, 38]; $P2X_7$: [39, 42–44]) in the murine PVZ. Ectonucleotidases, enzymes that are located at the cell surface and hydrolyze nucleotides to the respective nucleoside, have also been found in these areas [15]. The above evidence is almost exclusively based on mRNA and protein profiles. Pharmacological studies are almost completely missing, and the physiological relevance of the purinergic system in these brain regions is still elusive. Only two studies describe functional purinergic receptors in these brain regions. Astrocytes in the murine OB have been shown to express functional A_{2A} and $P2Y_1$ receptors [16], and cells of the PVZ of the murine lateral ventricles have been reported to express functional $P2X_7$ receptors [44]. Here, we set out to describe the organization of the PVZ of larval *X. laevis*, and to functionally characterize the purinergic system of the OB and its neurogenic PVZ. Our suggestions about the possible physiological roles of the purinergic system in these two brain areas should aid future work dealing with these topics.

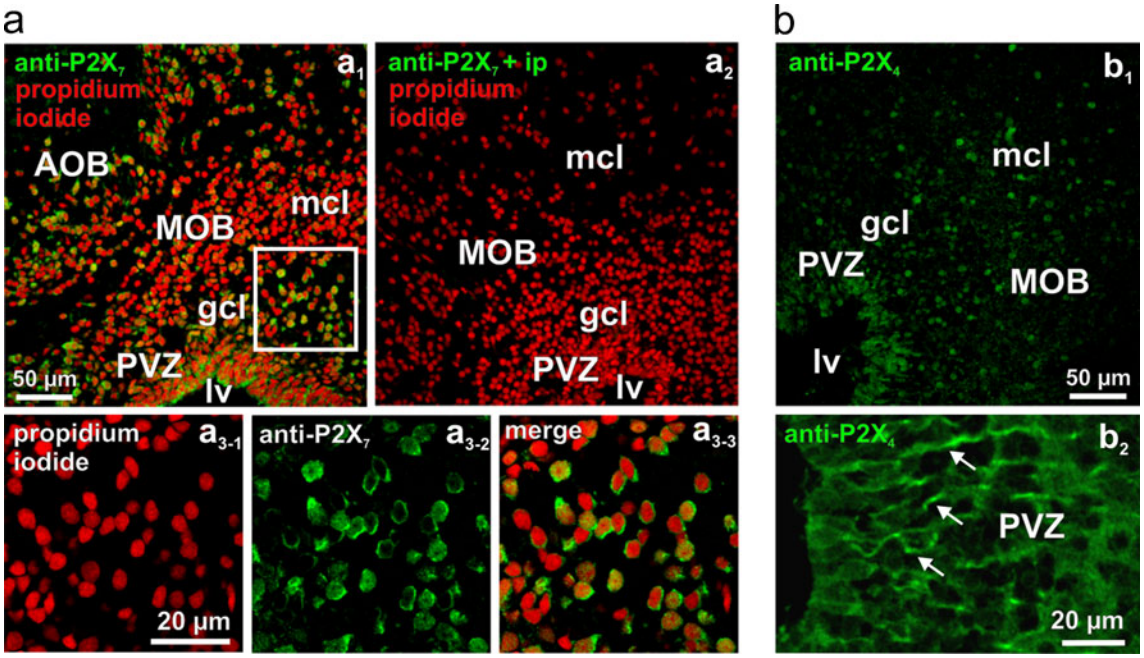

Fig. 7 Distribution of $P2X_7$- and $P2X_4$-like immunoreactivity in the anterior telencephalon. **a** Immunoreactivity to a $P2X_7$ antibody (*green fluorescence*) and cell nuclei staining with propidium iodide (*red fluorescence*) of a slice of the anterior telencephalon is shown in a_1. Another slice treated with the anti-$P2X_7$ antibody after preadsorption with the immunizing protein and counterstained with propidium iodide is shown in a_2. Higher magnification of the region indicated by the white rectangle in a_1 is shown in $a_{3\text{-}1}$–$a_{3\text{-}3}$. Note the clear somatic staining pattern of OB cells. **b** Immunoreactivity to a $P2X_4$ antibody (b_1) of another slice of the anterior telencephalon. Higher magnification of the $P2X_4$-like immunoreactivity of the PVZ (b_2). Note the stained tubular structures starting from the lateral ventricle and extending towards the OB (see arrows). Abbreviations: *MOB* main olfactory bulb, *AOB* accessory olfactory bulb, *PVZ* periventricular zone, *lv* lateral ventricle, *mcl* mitral cell layer, *gcl* granule cell layer

Ultrastructural analysis of the PVZ and quantification of the proliferation rate of its neuronal stem cells

Cells of the PVZ of the lateral ventricle have been shown to actively proliferate in larval *X. laevis* [4], and recent studies have identified these cells as true neuronal stem cells (reviewed in [3]). Nevertheless, the data describing the ultrastructure of the PVZ of the anterior telencephalon in larval *X. laevis* and amphibians in general is rather limited. In the present study, we set out to describe the architecture of this brain area and to get knowledge about the normal proliferation rate of its neuronal stem-/progenitor cells. The different morphology of the PVZ cells and the cells of the adjacent OB allowed to determine the borders between these two brain areas (see Fig. 1). This was very important for the further experiments of the present work. The PVZ of the anterior and medial part of the lateral ventricles consists of four to five cell layers with no apparent ependymal epithelium. This general appearance resembles that of the embryonic ventricular zone of higher vertebrates [45, 46]. In contrast, the PVZ situated laterally to the ventricle is thinner, with only one to two cell layers, resembling the typical ependymal ventricle lining present in adult higher vertebrates [45, 46]. The occurrence of mitotic cells and the presence of cells with chromatin in different states of aggregation showed that cells of the PVZ actively proliferate. Virtually all of the cells in close contact with the ventricular lumen are devoid of cilia or microvilli. In higher vertebrates, cells contacting the ventricular lumen have been shown to be ciliated [7, 8, 47]. Only very few cells in direct contact with the ventricles displayed a single cilium. Similar cells with a single primary cilium have been described in the adult ventricular zone of higher vertebrates. These cells have been reported to be related to radial glia, to actively proliferate and to produce new neurons and neuroblasts [7, 8]. The presence of large cytoplasmic expansions into the ventricular lumen and some multivesicular protrusions expanding into the ventricle suggest that cell material is releases into the lateral ventricles. Similar protrusions have been described in embryonic and adult cells lining the cerebral ventricles in several other species [48–50]. A more thorough description of the PVZ of larval *X. laevis* and a detailed classification of the different cell types populating this brain area was beyond the scope of this study. Future work will certainly bring more insight in the functional organization of the larval PVZ of this species.

To further identify the border between the PVZ and the OB and to quantify the proliferative capacity of the PVZ cells, we adopted a BrdU incorporation assay. It is known

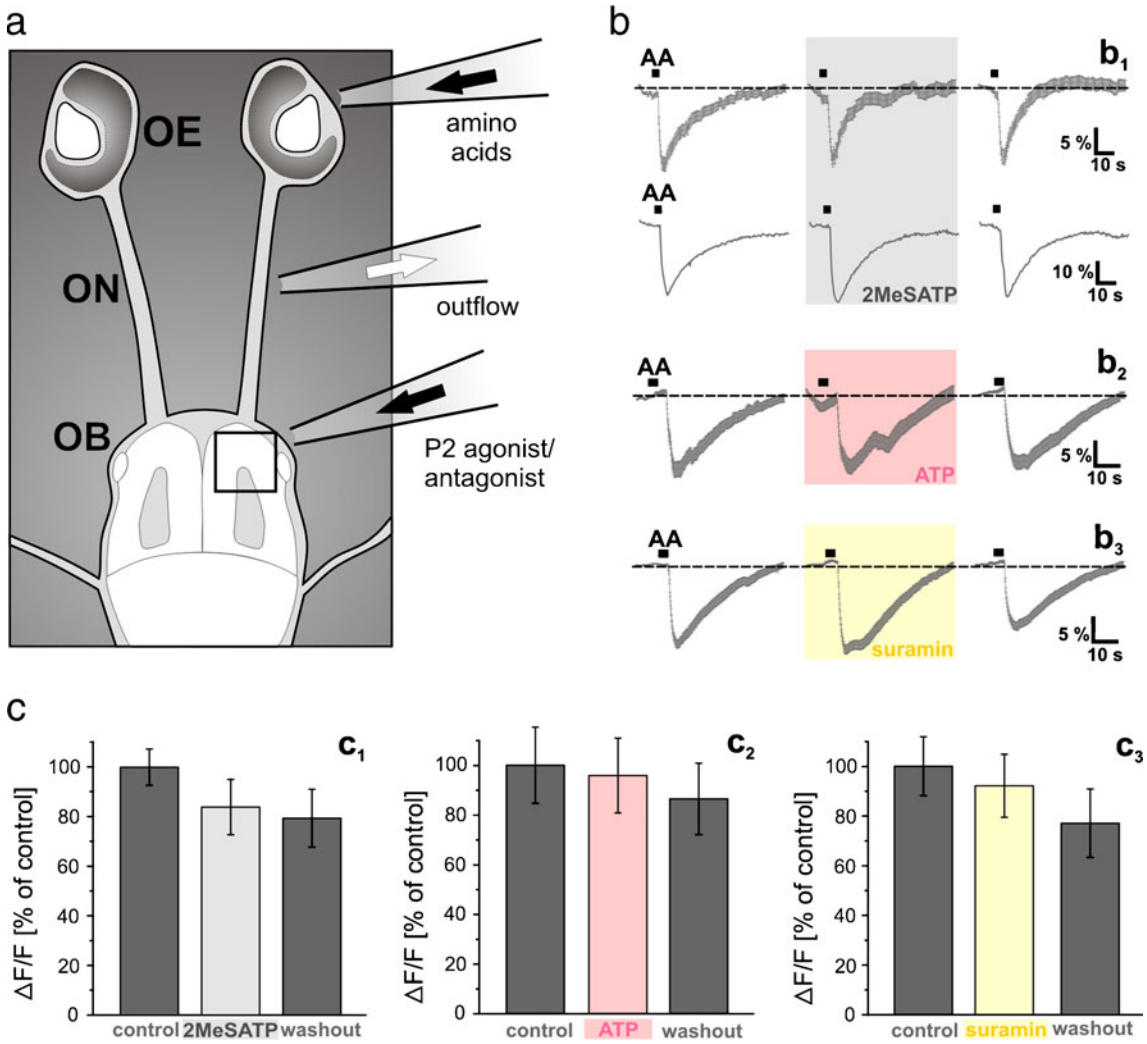

Fig. 8 Impact of the telencephalic purinergic system on the immediate processing of olfactory information in OB cells. **a** Schematic representation of a nose–brain preparation of larval *X. laevis*. The black rectangle indicates the area of the telencephalon monitored in the Ca^{2+} imaging experiments. **b** The mean response (±SEM) of all responsive cells of an OB (n=45 cells) upon epithelial application of an odorant mixture (15 amino acids, each at 100 μM; see "Materials and methods" section) was not affected by continuous OB stimulation with 5 μM 2MeSATP (b_1, *upper row*). Compare the trace in the *gray-shaded area* (amino acid-induced responses after 10 min of 2MeSATP perfusion) with the traces to its *left* (amino acid-induced responses prior to 2MeSATP perfusion) and *right* (amino acid-induced responses after 5 min washout of 2MeSATP). The *lower row* of b_1 shows the amino acid-induced $[Ca^{2+}]_i$ transient of a randomly chosen individual cell of the same slice. Also, the mean response (± SEM) of all amino acid-responsive cells of an OB (n=23 cells) was not affected by continuous OB stimulation with 100 μM ATP (b_2). Compare the trace in the *light red-shaded area* (amino acid-induced responses after 10 min of ATP perfusion) with the traces to its *left* (amino acid-induced responses prior to ATP perfusion) and *right* (amino acid-induced responses after 5 min washout of ATP). Prolonged application of 200 μM suramin did also not disrupt the mean response (±SEM) of all amino acid-responsive cells of an OB (n=35 cells; b_3). Compare the trace in the *yellow-shaded area* (amino acid-induced responses after 5 min of suramin perfusion) with the traces to its *left* (amino acid-induced responses prior to suramin perfusion) and *right* (amino acid-induced responses after 5 min washout of suramin). **c** The mean peak responses (±SEM), expressed as percent of control response to an epithelial application of 100 μM amino acid mixture (200 OB cells from four nose–brain preparations) in control conditions (*dark gray columns*) and after 5 to 10 min in bath solution with 5–20 μM 2MeSATP (*light gray column*) are shown in c_1. The mean peak responses ± SEM, expressed as percent of control response to an epithelial application of 100 μM amino acid mixture [78 OB cells/ 5 slices for ATP (100 μM) and 81 OB cells/4 slices for suramin 200 μM)] in control conditions (*dark gray columns*) and after 5 to 10 min in bath solution with ATP or suramin (*light red and yellow column*) are respectively given in c_2 and c_3. Abbreviations: *OE* olfactory epithelium, *ON* olfactory nerve, *OB* olfactory bulb, *AA* amino acid mixture

that proliferating cells actively incorporate BrdU [24]. Therefore, the location of BrdU-positive cells allowed an identification of the approximate borders between the two regions (see Fig. 2). We thereby chose an adequately long time window to stain enough cells in the PVZ, but not long enough to permit stained cells to migrate into the OB. Remarkably, more than 40% of the cells within the PVZ were BrdU-positive 24 h after the injection of BrdU. This

shows that the proliferation rate of neural stem/progenitor cells in larval *X. laevis* is extremely high.

Responses to nucleotides and functional investigation of the involved purinergic receptors

Application of 2MeSATP and ATP, two nucleotides known to activate many purinergic receptor subtypes [9], induced strong $[Ca^{2+}]_i$ increases in both, OB and PVZ cells. The fact that suramin and PPADS, two frequently used P2 receptor antagonists [9], attenuated these responses in both cell pools confirmed the involvement of purinergic receptors.

In the OB, glutamate mediates most or all excitatory synaptic interactions between the different cells populating this area of the brain via ionotropic receptors [1, 25]. Also, it has been reported that activation of purinergic receptors can induce neurotransmitter release, including glutamate, from neuronal [26, 27] and glial cells [26, 28, 29]. Therefore, we thought it would be necessary to exclude a possible contribution of ionotropic glutamate receptor activation, especially in the $[Ca^{2+}]_i$ increases recorded in cells of the OB. To do so, we compared ATP-induced $[Ca^{2+}]_i$ transients of cells of the anterior telencephalon, with and without the AMPA and NMDA receptor antagonist CNQX and APV in the bath solution. Blocking the ionotropic glutamate receptors did not significantly change the peak responses of cells of the anterior telencephalon.

To get a first indication of which receptor subtypes are involved, we investigated the effect of the omission of calcium from the extracellular solution. Although in Ca^{2+}-free bath solution the 2MeSATP- and ATP-induced $[Ca^{2+}]_i$ increases were significantly reduced in both brain regions, in all of the slices tested the reduction was consistently greater in the OB. While PVZ cells of all slices tested clearly retained some residual responses, in the vast majority of OB cells the responses were virtually abolished. This faint but clear difference between the two cell pools strongly suggested that the nucleotide-induced $[Ca^{2+}]_i$ increases were almost entirely due to activation of ionotropic P2X receptors in OB cells, while in the PVZ evidently a combination of ionotropic (P2X) and metabotropic purinergic receptors (P1 and/or P2Y receptors) contributed to the responses.

To verify this supposition and in the attempt to find clear differences in the purinergic receptor expression in the OB and the PVZ, we compared the efficacy of nine known purinergic agonists (see "Materials and methods" section). Significant differences could be observed with adenosine, ADP and ATP. Thereby, adenosine and ADP are particularly interesting. Both agonists were virtually inactive in the OB, while they induced considerable $[Ca^{2+}]_i$ increases in the PVZ. Although also ATP induced significantly stronger responses in cells of the PVZ, it is less adequate to differentiate between the two regions, as it induced strong responses also in the OB. α,β-MeATP and UTP were only very weakly active in both brain regions. β,γ-MeATP and uridine were completely inactive. 2MeSATP elicited strong but not significantly different $[Ca^{2+}]_i$ increases in cells of the OB and the PVZ. Also, BzATP elicited clear but not significantly different $[Ca^{2+}]_i$ increases in both brain regions, but it was apparently more effective in the OB.

The obtained agonist data does not allow to exactly identify the purinergic receptor subtypes involved in the Ca^{2+} signaling mechanisms in the anterior telencephalon of larval *X. laevis*, but it certainly allows a gross classification of the subtypes that are present in the different brain zones.

The virtually complete absence of 2MeSATP- and ATP-induced responses in Ca^{2+}-free extracellular solution together with the failure to elicit responses with adenosine, a selective P1 receptor agonist, strongly suggests that OB cells express almost exclusively ionotropic P2X receptors [9]. The very faint UTP- and ADP-mediated $[Ca^{2+}]_i$ increases could suggest a very weak expression of P2Y receptor subtypes [12, 51]. The presence of very few P2Y receptor subtypes on some cells of the OB could also explain the very faint residual nucleotide-induced responses in Ca^{2+}-free extracellular solution. The agonist responses of OB cells are not consistent with that reported for any of the seven known P2X subtypes [9, 10], suggesting that OB cells express multiple P2X subtypes. ATP, known to activate all known P2X receptor assemblies [10, 52, 53], was less potent than 2MeSATP. Already at concentrations of 5 to 10 μM 2MeSATP induced stronger responses than 50 μM ATP (Fig. 3b). This is an interesting result and apparently rather specific for the OB of larval *X. laevis*, as at most P2X subtypes in many species ATP is at least equipotent to 2MeSATP [9, 10, 52, 53]. BzATP, in turn, induced stronger responses than ATP. As BzATP has a higher potency than ATP only at the $P2X_7$ subtype [10, 52, 53], this result strongly suggest the presence of the $P2X_7$ subtype in the OB.

In contrast to the OB cells, cells of the PVZ consistently retained some residual 2MeSATP- and ATP-induced $[Ca^{2+}]_i$ transients in Ca^{2+}-free extracellular solution. This is a strong indication that in addition to ionotropic P2X subtypes, PVZ cells also express metabotropic purinergic receptors, known to be coupled to intracellular cascades linked to calcium release from internal stores [9, 12, 51]. The fact that also in the PVZ the omission of extracellular calcium in the bath solution significantly reduced the nucleotide-induced responses shows that the major fraction of purinergic receptors are P2X subtypes. On the other hand, the responses to adenosine, a selective agonist for P1 receptors [9, 54], nicely show that PVZ cells express also functional P1 receptors. 2MeSATP was the most potent agonist also in cells of the PVZ. The fact that responses to ADP were in the range of those to ATP suggests that PVZ cells express at least one P2Y subtype highly sensitive to

ADP [12, 51]. The faint UTP-mediated $[Ca^{2+}]_i$ increases in PVZ cells are also in line with the expression of P2Y subtypes [12, 51]. BzATP also induced clear responses in the PVZ. This could suggest that also PVZ cells express $P2X_7$ subtypes [52, 53], but also other P2X subtypes have been shown to be sensitive to BzATP [10, 12, 52, 53].

Immunohistochemical localization of purinergic receptors

We obtained positive $P2X_7$- and $P2X_4$-like stainings in the anterior telencephalon of larval *X. laevis*. No clear stainings were achieved with antibodies against $P2X_1$, $P2X_2$, $P2Y_2$, and $P2Y_4$ receptor subtypes. The antibody against the $P2X_7$ subtype gave a clear somatic staining pattern in both OB and PVZ cells. This result is in line with our calcium imaging data that strongly suggested the presence of the $P2X_7$ subtype. The successful $P2X_4$-like staining pattern suggests an expression of also this subtype. Thereby, the observed $P2X_4$-positive tubular structures starting from the ependymal layer of the lateral ventricle and extending through the PVZ into the OB could represent appendages of radial glia-like cells, or other proliferating precursor cells [6, 7, 55, 56]. These cells have been shown to possess a morphology resembling the observed structures [7, 55, 56]. This fits also very well to our observations of the ultrastructure of the PVZ, which suggested the presence of radial glia-like cells. As the used antibodies have been raised against rat P2 receptors, especially the negative results should be interpreted with caution. In the future, antibodies specifically raised against *X. laevis* purinergic receptors, in situ hybridization, or single-cell PCR experiments will hopefully provide a conclusive insight about the individual purinergic receptors subtypes expressed in the OB and the neurogenic PVZ.

Together, our pharmacological and immunohistochemical data clearly show that cells of the OB and the PVZ of larval *X. laevis* express purinergic receptors. We got strong evidence that OB cells almost exclusively express ionotropic P2X subtypes, and that cells of the PVZ most likely express a combination of ionotropic P2X and metabotropic P1 and P2Y subtypes. The exact identification of specific purinergic subtypes is inherently difficult, particularly in lower vertebrates such as amphibians. Nevertheless, the collective evidence of the present study permits a relatively clear survey of which purinergic receptor families are expressed in the anterior telencephalon, and more importantly revealed significant differences in the expression profile of purinergic receptors and the nucleotide-induced response behavior of cells of the OB and the PVZ. This knowledge will certainly aid future work dealing with questions regarding the physiological implication of the purinergic system in the anterior telencephalon of larval *X. laevis*.

On the physiological functions of the purinergic system in the anterior telencephalon

Olfactory bulb Long-term application of purinergic agonists and antagonists did not apparently modulate odorant-induced responses of OB cells. This strongly suggests that unlike other signaling systems, such as the noradrenergic or the GABAergic system (for a review see [25]), the purinergic system is most probably not involved in the immediate processing of olfactory information in the OB of larval *X. laevis*. Of course, more focused studies will be necessary to completely rule out an involvement of the purinergic system in the fine-tuning of olfactory information, but the results of the present study gave no indication in this direction. The presence of the $P2X_7$ subtype rather indicates that nucleotide-induced $[Ca^{2+}]_i$ signaling is involved in the sorting of bulbar interneurons. In the neuronal network of the OB a subset of interneurons are constantly renewed throughout the animals' life [1, 57], and cell death through apoptosis has been shown to play a crucial role in the lifelong cellular turnover [1, 58, 59]. On the other hand, perturbations of $[Ca^{2+}]_i$ have been shown to be involved in the initiation of cell death through apoptosis [60, 61], and the activation of the $P2X_7$ receptor has been brought into relation with the initiation of apoptosis in a variety of cells types [62, 63]. Among all purinergic receptors, the $P2X_7$ subtype has an interesting and unique characteristic. If activated briefly, it behaves like a non-selective cation channel, but a prolonged activation leads to the formation of a large non-selective pore permeable to molecules of up to 900 Da in size, including calcium [64]. It is therefore plausible that $P2X_7$ signaling is involved in the induction of apoptosis in OB cells that need to be sorted. To substantiate this assertion, future detailed studies focusing specifically on the involvement of this receptor in mechanisms regulating the cell turnover in the OB will be necessary.

Periventricular zone of the lateral ventricles Many molecules and their receptors have been shown to be involved in the regulation of neurogenesis [65, 66]. There is some evidence that also purinergic receptors might be involved (for a review, see [67]), but nucleotides to date are certainly among the least investigated groups of regulatory molecules. It is known that ependymal cells lining the murine ventricular system express purinergic receptors [14, 41, 42] and nucleotide-degrading enzymes [15]. It has also been shown that neurospheres derived from the adult mouse subventricular zone express metabotropic P2Y receptors and ectonucleotidases [68]. Application of nucleotides evoked fast $[Ca^{2+}]_i$ transients, and augmented cell proliferation in co-operation with growth factors [68]. Also neuronal progenitors of the subgranular zone are known to respond

to application of ATP, most probably via ionotropic P2X receptors [69, 70]. Another very recent study showed that cells of the PVZ along the lateral ventricle express functional $P2X_7$ receptors [44]. But the present study is the first detailed functional in situ analysis of the purinergic system of a vertebrate PVZ. We found evidence that PVZ cells of larval *X. laevis* express a complex web of purinergic receptor subtypes, and that application of nucleotides induces characteristic $[Ca^{2+}]_i$ transients in these cells. In various steps of the cell cycle $[Ca^{2+}]_i$ increases are important [71] and more specifically it is also known that $[Ca^{2+}]_i$ changes induced by P2Y receptor activation are essential for the transition from the G_1 to the S and M phases of the cell cycle [72]. It might therefore be speculated that nucleotide-induced $[Ca^{2+}]_i$ changes in neurogenic brain areas are deeply involved in the control of the proliferation of neuronal stem cells. The finding that P1, P2X as well as P2Y purinergic receptor subtypes are present in the PVZ of larval *X. laevis*, suggests that different nucleosides and nucleotides are likely involved in the fine-tuning of neuronal differentiation. Future detailed studies, specifically focusing on the interplay of the different purinergic receptor subtypes, but also on the interplay of the purinergic system with other regulatory systems will certainly bring more insight.

As a last point, we would like to focus on the anatomical difference in the location of the telencephalic neurogenic areas between *X. laevis* and higher vertebrates. In embryos and adults of higher vertebrates, such as mammals, OB interneurons derive from a neuronal precursor cell pool situated at a certain distance from the OB. In embryos, interneurons migrate into the OB from the lateral ganglionic eminence. In adults, they derive from the subventricular zone and migrate to the OB following the rostral migratory stream. In some species, neuronal precursor cells have to cover distances up to several centimeters to reach the OB (for a review see [1]). In *X. laevis* a neuronal precursor cell pool directly borders the OB. Newborn interneurons can readily be integrated into the OB without traveling long distances. This anatomic peculiarity could certainly be of advantage for future studies dealing with basic mechanisms involved in the regulation of neurogenesis in general and the neuronal turnover in the OB in particular. In this context, it will of course be essential to investigate whether the purinergic system of the anterior telencephalon persists also in adult *X. laevis*, and whether in the adult system it is involved in the same physiological processes as in the larvae.

Acknowledgments This work was supported by grants from the Research program, Faculty of Medicine, Georg-August-University Göttingen to I.M., and the DFG Research Center for Molecular Physiology of the Brain (CMPB, Project B1/9) to I.M. and D.S.

References

1. Lledo PM, Gheusi G, Vincent JD (2005) Information processing in the mammalian olfactory system. Physiol Rev 85:281–317
2. Hildebrand JG, Shepherd GM (1997) Mechanisms of olfactory discrimination: converging evidence for common principles across phyla. Annu Rev Neurosci 20:595–631
3. Endo T, Yoshino J, Kado K, Tochinai S (2007) Brain regeneration in anuran amphibians. Dev Growth Differ 49:121–129
4. Filoni S, Bernardini S, Cannata SM (1995) Differences in the decrease in regenerative capacity of various brain regions of *Xenopus laevis* are related to differences in the undifferentiated cell populations. J Hirnforsch 36:523–529
5. Chojnacki AK, Mak GK, Weiss S (2009) Identity crisis for adult periventricular neural stem cells: subventricular zone astrocytes, ependymal cells or both? Nat Rev Neurosci 10:153–163
6. Tramontin AD, Garcia-Verdugo JM, Lim DA, Alvarez-Buylla A (2003) Postnatal development of radial glia and the ventricular zone (VZ): a continuum of the neural stem cell compartment. Cereb Cortex 13:580–587
7. Kriegstein A, Alvarez-Buylla A (2009) The glial nature of embryonic and adult neural stem cells. Annu Rev Neurosci 32:149–184
8. Mirzadeh Z, Merkle FT, Soriano-Navarro M, Garcia-Verdugo JM, Alvarez-Buylla A (2008) Neural stem cells confer unique pinwheel architecture to the ventricular surface in neurogenic regions of the adult brain. Cell Stem Cell 3:265–278
9. Ralevic V, Burnstock G (1998) Receptors for purines and pyrimidines. Pharmacol Rev 50:413–492
10. Khakh BS, Burnstock G, Kennedy C, King BF, North RA, Seguela P, Voigt M, Humphrey PP (2001) International union of pharmacology. XXIV. Current status of the nomenclature and properties of P2X receptors and their subunits. Pharmacol Rev 53:107–118
11. Prinster SC, Hague C, Hall RA (2005) Heterodimerization of g protein-coupled receptors: specificity and functional significance. Pharmacol Rev 57:289–298
12. Abbracchio MP, Burnstock G, Boeynaems JM, Barnard EA, Boyer JL, Kennedy C, Knight GE, Fumagalli M, Gachet C, Jacobson KA, Weisman GA (2006) International Union of Pharmacology LVIII: update on the P2Y G protein-coupled nucleotide receptors: from molecular mechanisms and pathophysiology to therapy. Pharmacol Rev 58:281–341
13. Bogdanov YD, Dale L, King BF, Whittock N, Burnstock G (1997) Early expression of a novel nucleotide receptor in the neural plate of *Xenopus* embryos. J Biol Chem 272:12583–12590
14. Burnstock G, Knight GE (2004) Cellular distribution and functions of P2 receptor subtypes in different systems. Int Rev Cytol 240:31–304
15. Langer D, Hammer K, Koszalka P, Schrader J, Robson S, Zimmermann H (2008) Distribution of ectonucleotidases in the rodent brain revisited. Cell Tissue Res 334:199–217
16. Doengi M, Deitmer JW, Lohr C (2008) New evidence for purinergic signaling in the olfactory bulb: A2A and P2Y1 receptors mediate intracellular calcium release in astrocytes. FASEB J 22:2368–2378
17. Nieuwkoop PD, Faber J (1994) Normal table of *Xenopus laevis* (Daudin).

18. Manzini I, Rössler W, Schild D (2002) cAMP-independent responses of olfactory neurons in *Xenopus laevis* tadpoles and their projection onto olfactory bulb neurons. J Physiol 545:475–484
19. Czesnik D, Rössler W, Kirchner F, Gennerich A, Schild D (2003) Neuronal representation of odourants in the olfactory bulb of *Xenopus laevis* tadpoles. Eur J Neurosci 17:113–118
20. Manzini I, Schild D (2003) cAMP-independent olfactory transduction of amino acids in *Xenopus laevis* tadpoles. J Physiol 551:115–123
21. Manzini I, Schweer TS, Schild D (2008) Improved fluorescent (calcium indicator) dye uptake in brain slices by blocking multidrug resistance transporters. J Neurosci Methods 167:140–147
22. Hassenklöver T, Kurtanska S, Bartoszek I, Junek S, Schild D, Manzini I (2008) Nucleotide-induced Ca^{2+} signaling in sustentacular supporting cells of the olfactory epithelium. Glia 56:1614–1624
23. Carpenter AE, Jones TR, Lamprecht MR, Clarke C, Kang IH, Friman O, Guertin DA, Chang JH, Lindquist RA, Moffat J, Golland P, Sabatini DM (2006) CellProfiler: image analysis software for identifying and quantifying cell phenotypes. Genome Biol 7:R100-
24. Taupin P (2007) BrdU immunohistochemistry for studying adult neurogenesis: paradigms, pitfalls, limitations, and validation. Brain Res Rev 53:198–214
25. Shipley MT, Ennis M (1996) Functional organization of olfactory system. J Neurobiol 30:123–176
26. Burnstock G (2007) Physiology and pathophysiology of purinergic neurotransmission. Physiol Rev 87:659–797
27. Gu JG, MacDermott AB (1997) Activation of ATP P2X receptors elicits glutamate release from sensory neuron synapses. Nature 389:749–753
28. Jeremic A, Jeftinija K, Stevanovic J, Glavaski A, Jeftinija S (2001) ATP stimulates calcium-dependent glutamate release from cultured astrocytes. J Neurochem 77:664–675
29. Malarkey EB, Parpura V (2008) Mechanisms of glutamate release from astrocytes. Neurochem Int 52:142–154
30. Abbracchio MP, Burnstock G, Verkhratsky A, Zimmermann H (2009) Purinergic signalling in the nervous system: an overview. Trends Neurosci 32:19–29
31. Vulchanova L, Arvidsson U, Riedl M, Wang J, Buell G, Surprenant A, North RA, Elde R (1996) Differential distribution of two ATP-gated channels (P2X receptors) determined by immunocytochemistry. Proc Natl Acad Sci USA 93:8063–8067
32. Kanjhan R, Housley GD, Burton LD, Christie DL, Kippenberger A, Thorne PR, Luo L, Ryan AF (1999) Distribution of the P2X2 receptor subunit of the ATP-gated ion channels in the rat central nervous system. J Comp Neurol 407:11–32
33. Hegg CC, Greenwood D, Huang W, Han P, Lucero MT (2003) Activation of purinergic receptor subtypes modulates odor sensitivity. J Neurosci 23:8291–8301
34. Bo X, Zhang Y, Nassar M, Burnstock G, Schoepfer R (1995) A P2X purinoceptor cDNA conferring a novel pharmacological profile. FEBS Lett 375:129–133
35. Collo G, North RA, Kawashima E, Merlo-Pich E, Neidhart S, Surprenant A, Buell G (1996) Cloning OF P2X5 and P2X6 receptors and the distribution and properties of an extended family of ATP-gated ion channels. J Neurosci 16:2495–2507
36. Le KT, Villeneuve P, Ramjaun AR, McPherson PS, Beaudet A, Seguela P (1998) Sensory presynaptic and widespread somatodendritic immunolocalization of central ionotropic P2X ATP receptors. Neuroscience 83:177–190
37. Guo W, Xu X, Gao X, Burnstock G, He C, Xiang Z (2008) Expression of P2X5 receptors in the mouse CNS. Neuroscience 156:673–692
38. Soto F, Garcia-Guzman M, Karschin C, Stühmer W (1996) Cloning and tissue distribution of a novel P2X receptor from rat brain. Biochem Biophys Res Commun 223:456–460
39. Yu Y, Ugawa S, Ueda T, Ishida Y, Inoue K, Kyaw NA, Umemura A, Mase M, Yamada K, Shimada S (2008) Cellular localization of P2X7 receptor mRNA in the rat brain. Brain Res 1194:45–55
40. Simon J, Webb TE, Barnard EA (1997) Distribution of [35S]dATP alpha S binding sites in the adult rat neuraxis. Neuropharmacology 36:1243–1251
41. Worthington RA, Arumugam TV, Hansen MA, Balcar VJ, Barden JA (1999) Identification and localisation of ATP P2X receptors in rat midbrain. Electrophoresis 20:2077–2080
42. Collo G, Neidhart S, Kawashima E, Kosco-Vilbois M, North RA, Buell G (1997) Tissue distribution of the P2X7 receptor. Neuropharmacology 36:1277–1283
43. Sim JA, Young MT, Sung HY, North RA, Surprenant A (2004) Reanalysis of P2X7 receptor expression in rodent brain. J Neurosci 24:6307–6314
44. Genzen JR, Platel JC, Rubio ME, Bordey A (2009) Ependymal cells along the lateral ventricle express functional P2X(7) receptors. Purinergic Signal 5:299–307
45. Takahashi T, Nowakowski RS, Caviness VS Jr (1995) The cell cycle of the pseudostratified ventricular epithelium of the embryonic murine cerebral wall. J Neurosci 15:6046–6057
46. Takahashi T, Nowakowski RS, Caviness VS Jr (1996) Interkinetic and migratory behavior of a cohort of neocortical neurons arising in the early embryonic murine cerebral wall. J Neurosci 16:5762–5776
47. Garcia-Verdugo JM, Ferron S, Flames N, Collado L, Desfilis E, Font E (2002) The proliferative ventricular zone in adult vertebrates: a comparative study using reptiles, birds, and mammals. Brain Res Bull 57:765–775
48. Wittkowski W (1969) Ependymal secretion and receptors in the wall of the recessus infundibularis in mice and their relationship to the small-cell hypothalamus. Z Zellforsch Mikrosk Anat 93:530–546
49. Nakai Y (1971) Fine structure and its functional properties of the ependymal cell in the frog median eminence. Z Zellforsch Mikrosk Anat 122:15–25
50. Hetzel W (1978) Ependyma and ependymal protrusions of the lateral ventricles of the rabbit brain. Cell Tissue Res 192:475–488
51. von Kügelgen I (2006) Pharmacological profiles of cloned mammalian P2Y-receptor subtypes. Pharmacol Ther 110:415–432
52. North RA (2002) Molecular physiology of P2X receptors. Physiol Rev 82:1013–1067
53. Gever JR, Cockayne DA, Dillon MP, Burnstock G, Ford AP (2006) Pharmacology of P2X channels. Pflugers Arch 452:513–537
54. Fredholm BB, IJzerman AP, Jacobson KA, Klotz KN, Linden J (2001) International Union of Pharmacology. XXV. Nomenclature and classification of adenosine receptors. Pharmacol Rev 53:527–552
55. Zhao C, Teng EM, Summers RG Jr, Ming GL, Gage FH (2006) Distinct morphological stages of dentate granule neuron maturation in the adult mouse hippocampus. J Neurosci 26:3–11
56. Bonfanti L, Peretto P (2007) Radial glial origin of the adult neural stem cells in the subventricular zone. Prog Neurobiol 83:24–36
57. Alvarez-Buylla A, Garcia-Verdugo JM, Tramontin AD (2001) A unified hypothesis on the lineage of neural stem cells. Nat Rev Neurosci 2:287–293
58. Petreanu L, Alvarez-Buylla A (2002) Maturation and death of adult-born olfactory bulb granule neurons: role of olfaction. J Neurosci 22:6106–6113
59. Winner B, Cooper-Kuhn CM, Aigner R, Winkler J, Kuhn HG (2002) Long-term survival and cell death of newly generated neurons in the adult rat olfactory bulb. Eur J Neurosci 16:1681–1689
60. Orrenius S, Zhivotovsky B, Nicotera P (2003) Regulation of cell death: the calcium-apoptosis link. Nat Rev Mol Cell Biol 4:552–565

61. Berliocchi L, Bano D, Nicotera P (2005) Ca^{2+} signals and death programmes in neurons. Philos Trans R Soc Lond B Biol Sci 360:2255–2258
62. Chow SC, Kass GE, Orrenius S (1997) Purines and their roles in apoptosis. Neuropharmacology 36:1149–1156
63. Di Virgilio F, Chiozzi P, Falzoni S, Ferrari D, Sanz JM, Venketaraman V, Baricordi OR (1998) Cytolytic P2X purinoceptors. Cell Death Differ 5:191–199
64. Virginio C, MacKenzie A, Rassendren FA, North RA, Surprenant A (1999) Pore dilation of neuronal P2X receptor channels. Nat Neurosci 2:315–321
65. Grote HE, Hannan AJ (2007) Regulators of adult neurogenesis in the healthy and diseased brain. Clin Exp Pharmacol Physiol 34:533–545
66. Hagg T (2005) Molecular regulation of adult CNS neurogenesis: an integrated view. Trends Neurosci 28:589–595
67. Zimmermann H (2006) Nucleotide signaling in nervous system development. Pflugers Arch 452:573–588
68. Mishra SK, Braun N, Shukla V, Fullgrabe M, Schomerus C, Korf HW, Gachet C, Ikehara Y, Sevigny J, Robson SC, Zimmermann H (2006) Extracellular nucleotide signaling in adult neural stem cells: synergism with growth factor-mediated cellular proliferation. Development 133:675–684
69. Shukla V, Zimmermann H, Wang L, Kettenmann H, Raab S, Hammer K, Sevigny J, Robson SC, Braun N (2005) Functional expression of the ecto-ATPase NTPDase2 and of nucleotide receptors by neuronal progenitor cells in the adult murine hippocampus. J Neurosci Res 80:600–610
70. Hogg RC, Chipperfield H, Whyte KA, Stafford MR, Hansen MA, Cool SM, Nurcombe V, Adams DJ (2004) Functional maturation of isolated neural progenitor cells from the adult rat hippocampus. Eur J Neurosci 19:2410–2420
71. Santella L, Ercolano E, Nusco GA (2005) The cell cycle: a new entry in the field of Ca^{2+} signaling. Cell Mol Life Sci 62:2405–2413
72. Miyagi Y, Kobayashi S, Ahmed A, Nishimura J, Fukui M, Kanaide H (1996) P2U purinergic activation leads to the cell cycle progression from the G1 to the S and M phases but not from the G0 to G1 phase in vascular smooth muscle cells in primary culture. Biochem Biophys Res Commun 222:652–658